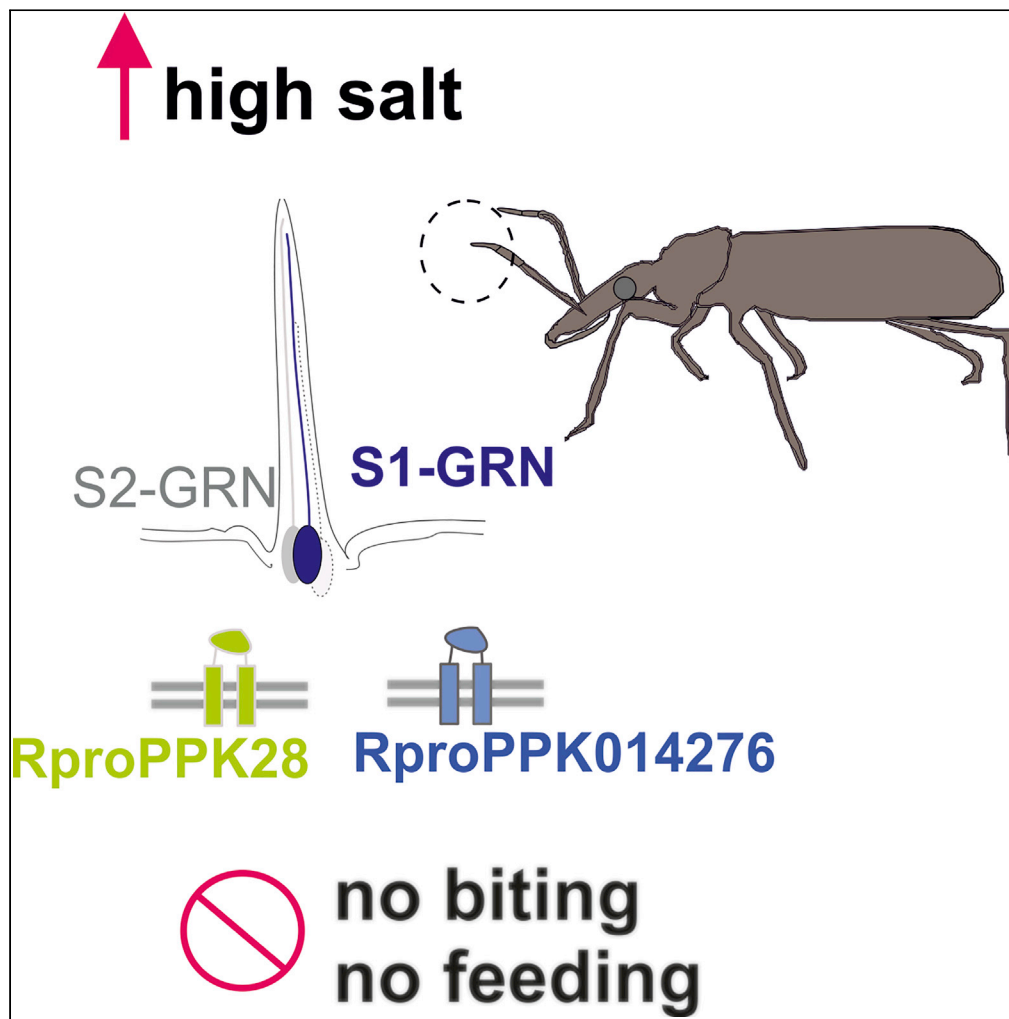


## Article

## Molecular and functional basis of high-salt avoidance in a blood-sucking insect



Gina Pontes, José Manuel Latorre-Estivalis, María Laura Gutiérrez, Agustina Cano, Martín Berón de Astrada, Marcelo G. Lorenzo, Romina B. Barrozo

rbarrozo@bg.fcen.uba.ar

**Highlights**

High-salt sensing prevents biting and feeding in a blood-sucking insect

High-salt avoidance is mediated by an antennal gustatory receptor neuron

Two PPK receptors, *RproPPK014276* and *RproPPK28*, are required for high-salt detection

*RproPPK014276* and *RproPPK28* are sensitive to amiloride blockade

## Article

## Molecular and functional basis of high-salt avoidance in a blood-sucking insect

Gina Pontes,<sup>1,4</sup> José Manuel Latorre-Estivalis,<sup>2,4,5</sup> María Laura Gutiérrez,<sup>1,4</sup> Agustina Cano,<sup>1</sup> Martin Berón de Astrada,<sup>3</sup> Marcelo G. Lorenzo,<sup>2</sup> and Romina B. Barrozo<sup>1,6,\*</sup>

## SUMMARY

**Salts are essential nutrients required for many physiological processes, and accordingly, their composition and concentration are tightly regulated. Taste is the ultimate sensory modality involved in resource quality assessment, resulting in acceptance or rejection. Here we found that high salt concentrations elicit feeding avoidance in the blood-sucking bug *Rhodnius prolixus* and elucidate the molecular and neurophysiological mechanisms involved. We found that high-salt avoidance is mediated by a salt-sensitive antennal gustatory receptor neuron (GRN). Using RNAi, we demonstrate that this process requires two amiloride-sensitive pickpocket channels (PPKs; *RproPPK014276* and *RproPPK28*) expressed within these cells. We found that antennal GRNs project to the insect primary olfactory center, the antennal lobes, revealing these centers as potential sites for the integration of taste and olfactory host-derived cues. Moreover, the identification of the gustatory basis of high-salt detection in a hematophagous insect suggests novel targets for the prevention of biting and feeding.**

## INTRODUCTION

Salts are vital for physiological processes. Sodium and potassium chloride regulation to adequate levels are crucial for maintaining electrolyte homeostasis and neuronal transmission. Deficient or excessive salt results in adverse health effects. Consequently, in most animals studied so far, the assessment of salt concentration drives behavioral acceptance or avoidance responses (Liman et al., 2014; Yarmolinsky et al., 2009). For example, low salt (<0.1 M) triggers insect feeding and oviposition, whereas high salt (>0.2 M) promotes feeding avoidance and prevents egg-laying (Cano et al., 2017; Liu et al., 2003; Matthews et al., 2019; Newland and Yates, 2008; Niewalda et al., 2008; Pontes et al., 2017; Zhang et al., 2013). Salts are detected by the taste system, a sensory modality that helps animals make predictions about the value of a potential food source, i.e. it might be beneficial or harmful. Found on the body surface of insects (Liman et al., 2014), taste sensilla are the structural units of this system that house gustatory receptor neurons (GRNs). GRNs carry specific receptors on their dendritic membrane that favor the detection of different types of gustatory stimuli (Freeman and Dahanukar, 2015). Upon GRN stimulation, a message is sent to the brain through action potentials and, consequently, the appropriate behavior is set into motion: biting or not, eating or not.

Despite the relevance of salts to many life traits in animals, the molecular and physiological mechanisms underlying low and high salt detection and processing are not well understood (Jaeger et al., 2018; Roper, 2015). Degenerin-epithelium sodium channels (DEG/ENaC) have been related to salt sensing in mammals (Chandrashekar et al., 2010). Insect pickpocket channel receptors (PPK) belong to the DEG/ENaC family and were reported to detect salt in *Drosophila melanogaster*, among other functions (Zelle et al., 2013). They constitute a large family of ligand-gated membrane proteins, voltage-insensitive ion channels, and some of them are highly sensitive to amiloride (AMI) blockade (Ben-Shahar, 2011; Kellenberger and Schild, 2002). The *DmelPPK11* and *DmelPPK19* genes, for example, were related to low-salt detection in the fruit fly *D. melanogaster* (Liu et al., 2003). Besides, fruit fly *DmelPPK28* and its mosquito orthologue *AegPPK301* (*Aedes aegypti*) were identified as osmolarity sensors because the GRNs expressing them respond to hypo-osmotic solutions (Cameron et al., 2010; Chen et al., 2010; Matthews et al., 2019). High-salt sensing in *D. melanogaster*, on the other hand, occurs through specific GRNs that also detect bitter compounds (Hiroi et al., 2004) and a population of glutamatergic neurons expressing *DmelPPK23* (Jaeger et al.,

<sup>1</sup>Grupo de Neuroetología de Insectos Vectores, Laboratorio Fisiología de Insectos, Instituto de Biodiversidad, Biología Experimental y Aplicada, CONICET - UBA, Departamento Biodiversidad y Biología Experimental, Facultad Ciencias Exactas y Naturales, Universidad de Buenos Aires, Buenos Aires, Argentina

<sup>2</sup>Grupo de Comportamento de Vetores e Interação com Patógenos-CNPq, Centro de Pesquisas René Rachou/FIOCRUZ, Belo Horizonte, Brazil

<sup>3</sup>Laboratorio de Fisiología de la Visión, Instituto de Biociencias, Biotecnología y Biología Traslacional, Departamento de Fisiología, Biología Molecular y Celular, Facultad Ciencias Exactas y Naturales, Universidad de Buenos Aires, CONICET, Buenos Aires, Argentina

<sup>4</sup>These authors contributed equally

<sup>5</sup>Present address: Laboratorio de Insectos Sociales, Instituto de Fisiología, Biología Molecular y Neurociencias, Instituto de Fisiología, Biología Molecular y Neurociencias, CONICET - UBA, Facultad Ciencias Exactas y Naturales, Universidad de Buenos Aires, Buenos Aires, Argentina

<sup>6</sup>Lead contact

\*Correspondence: rbarrozo@bg.fcen.uba.ar  
<https://doi.org/10.1016/j.isci.2022.104502>



2018). However, the detection of salt seems complex and, in addition to PPKs, other receptors also participate, such as *IR76b*, *IR94e*, and *sano* (Alves et al., 2014; Jaeger et al., 2018; Lee et al., 2017).

In blood-feeding insects, salts such as NaCl and KCl were demonstrated to be relevant gustatory cues in a feeding context (Barrozo, 2019; Friend and Smith, 1977), probably because salts are essential components of the blood of vertebrates. Besides, salts are found on human skin as part of sweat, a product of the eccrine glands' excretion (Baker and Wolfe, 2020; Buono et al., 2007; Cage and Dobson, 1965). Salt concentration modulates the behavior of the hematophagous bug *Rhodnius prolixus*, triggering avoidance or preference responses. For example, they avoid walking over surfaces coated with high-NaCl or -KCl (1 M) while preferred those added with low-NaCl or KCl (0.1 M) (Masagué et al., 2020; Minoli et al., 2018). Furthermore, *R. prolixus* accepts feeding on an artificial solution containing a NaCl concentration similar to that of the vertebrate plasma (0.15 M), while refusing if it is above this level ( $\geq 0.2$  M) (Cano et al., 2017; Pontes et al., 2017). Many molecules produce insect avoidance due to the negative impact they may have on their physiology, i.e. toxic or even lethal effects (Chapman, 2003; Muñoz et al., 2020). Therefore, biting and feeding decisions depend strongly on the assessment of the chemical qualities of the food source. The stereotypic avoidance responses produced by high-salt perception could represent a valuable tool to be exploited in the control of insect vectors. Still, the mechanism behind high-salt sensing in blood-feeding insects has been completely unexplored. In this work, we asked if detection of high-salt levels over the host skin or a substrate could prevent insect biting and feeding. Moreover, we investigated the underlying molecular, cellular, pharmacological, neuroanatomical, and physiological mechanisms for high-salt sensing in the hematophagous insect *R. prolixus*.

Triatomine insects (Hemiptera: Reduviidae), commonly known as kissing bugs, are vectors of the protozoan parasite *Trypanosoma cruzi*, causing Chagas disease in humans. Whereas Chagas disease is considered endemic to Mexico, Central, and South America, it has become a global health problem affecting an increasing number of nonendemic countries (Edwards et al., 2017; World Health Organization, 2020). In the United States of America, the Center for Disease Control and Prevention (CDC) considered Chagas disease as one of the five neglected parasitic infections to be targeted as a priority for public health (Mutebi et al., 2017).

Our results show that detection of high-salt biting substrates results in feeding avoidance. We found that two amiloride-sensitive pickpocket channel receptors (PPKs; *RproPPK014276* and *RproPPK28*) expressed in an antennal salt-sensitive GRN drive high-salt avoidance. Besides, we show that antennal GRNs project to the antennal lobes (a brain region mostly dedicated to the processing of olfactory information in insects), where the antennal gustatory information seems to be processed in *R. prolixus*.

## RESULTS

### High-salt bite sites prevent feeding

Kissing bugs assess the quality of a potential food source by tasting the host skin (Pontes et al., 2014). Consequently, we asked whether detection of high salt above the bite site would affect feeding on an otherwise appetitive solution (AS). To do this, the membrane of the artificial feeder mimicking the host skin was coated with different concentrations of NaCl (Na) or KCl (K): no-Na/no-K, low-Na/low-K, mid-Na/mid-K, or high-Na/high-K (Figure 1A). Note that no-Na and no-K represent control groups, in which the membrane was impregnated with distilled water instead of a salt solution.

Insects fed on low-Na- or low-K-coated membranes of the artificial feeder, as did those tested on the control membrane (no-Na/no-K, Figure 1A). Thus, the low-salt addition on the bite site did not improve or decrease the feeding behavior of insects. In contrast, a significant reduction in the percentage of insects feeding on the AS was observed when the bite membrane was coated with mid-Na or high-Na/high-K ( $p < 0.01$ ). Despite the apparent difference in the percentage of insects that fed on Na and K coated membranes (Figure 1A), no statistical differences were detected among curves (n.s.).

Biting and feeding activities are closely associated; this was evident by registering in parallel the percentage of insects that bit and fed on a salt-free membrane and a high-salt-coated membrane of the feeder. No significant differences were detected between biting and feeding events (Figure S1), and a reduction in biting to high-Na was translated in a concomitant decrease in feeding. Therefore, high-salt perception on the bite site produces both biting and feeding avoidance in *R. prolixus*.

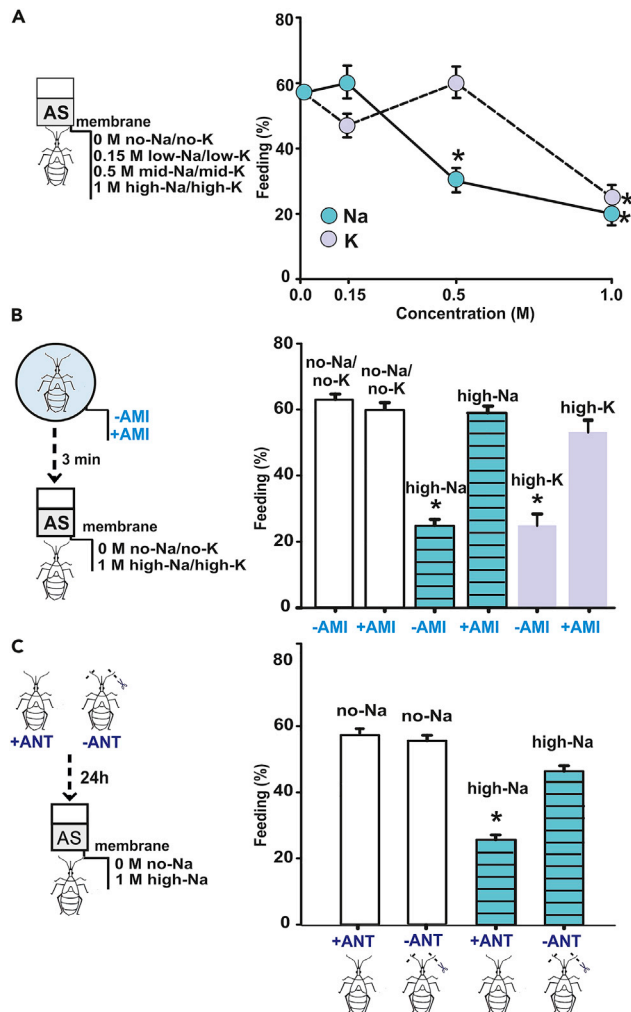


**Figure 1. High-salt bite substrates trigger feeding avoidance**

(A) Increasing salt concentration on the bite membrane prevents feeding. The bite membrane was coated with no-Na/no-K (0 M), low-Na/low-K (0.15 M), mid-Na/mid-K (0.5 M), or high-Na/high-K (1 M). Dots represent the percentage ( $\pm$  SEM) of fed insects. Insects avoided feeding after contacting membranes coated with mid-Na or high-Na/high-K. Asterisks indicate, for each salt, significant differences across concentrations (Pearson  $X^2$ ,  $k = 3$ ,  $\alpha' = 0.016$ ,  $p < 0.01$ ); 20 to 36 replicates were carried out.

(B) Amiloride blocks high-salt feeding avoidance. Insects were pretreated with amiloride (+AMI) or distilled water (–AMI). Three minutes later insects were exposed to membranes coated with no-Na/no-K (0 M) or with high-Na/high-K (1 M). Bars represent the percentage ( $\pm$  SEM) of fed insects. Amiloride blocked high-Na/high-K perception and insects fed over high-Na/high-K coated membranes. Asterisks indicate, for each salt, significant differences among all groups (Pearson  $X^2$ ,  $k = 3$ ,  $\alpha' = 0.016$ ,  $p < 0.01$ ); 20 to 32 replicates were carried out for each experimental condition.

(C) Intact antennae are required for high-salt feeding avoidance. The distal tips of the antennal flagellomeres were ablated (–ANT) or kept intact (+ANT). Twenty-four hours later insects were exposed to membranes coated with no-Na (0 M) or with high-Na (1 M). Bars represent the percentage ( $\pm$  SEM) of fed insects. In the absence of the taste sensilla on the antennal flagellomeres, insects fed despite the high-Na-coated membranes. The asterisk indicates a significant difference among all groups (Pearson  $X^2$ ,  $k = 3$ ,  $\alpha' = 0.016$ ,  $p < 0.01$ ); 30 replicates were carried out for each treatment.

### High-salt avoidance is impaired by amiloride blockade

DEG/ENaCs, including insect PPKs receptors, can be blocked by amiloride (Chen et al., 2010; Halpern, 1998; Jenkins and Tompkins, 1990; Liu et al., 2003). Therefore, we examined whether this drug could block the detection of high salt during bite site assessment by kissing bugs. To test this, insects were exposed to amiloride (+AMI) or distilled water (–AMI). Following the treatment, feeding responses to the AS on coated membranes with no-Na/no-K or a high-Na/high-K were evaluated (Figure 1B).

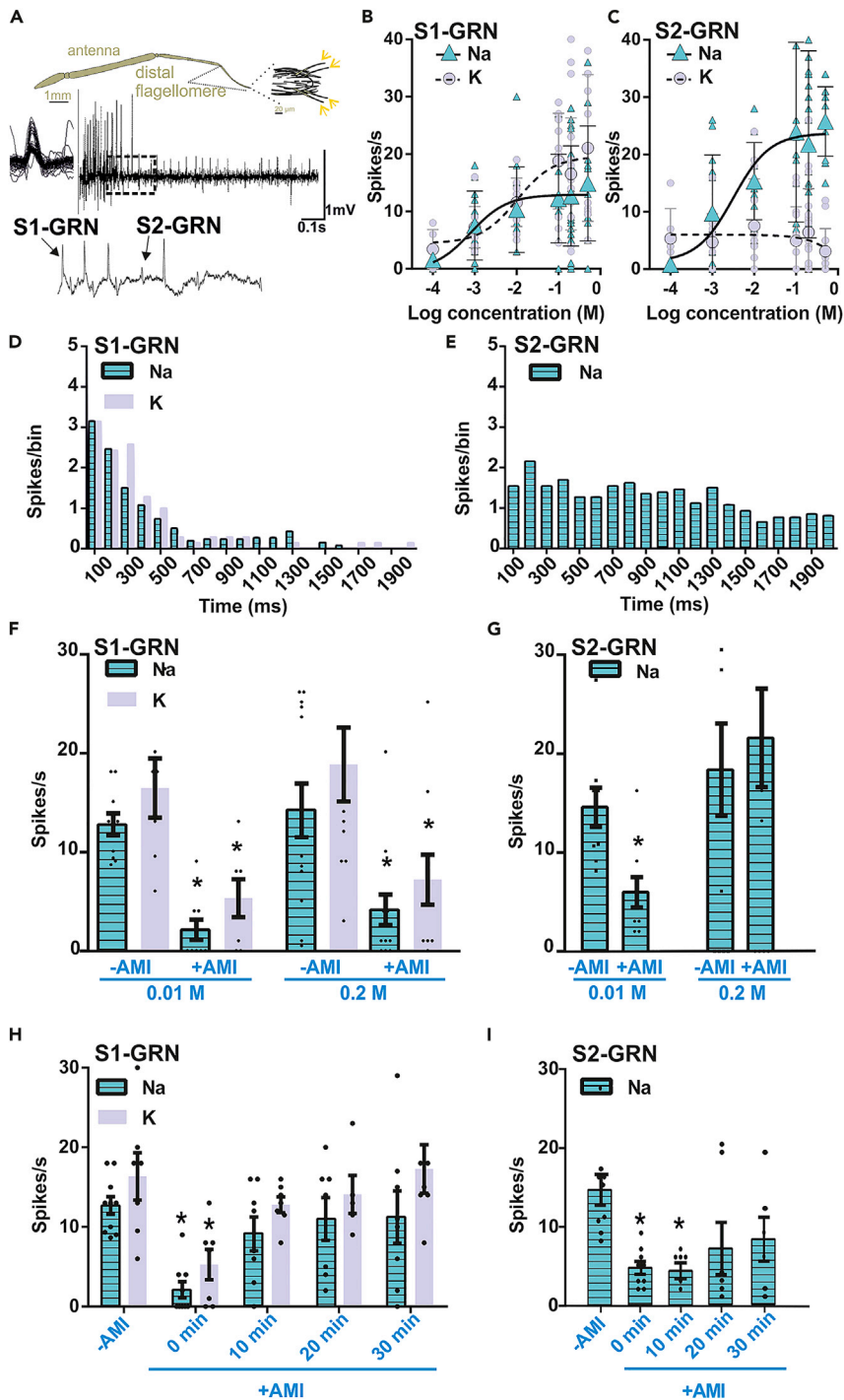


**Figure 2. Antennal gustatory receptor neurons involved in salt detection**

(A) Scheme of the antenna of *R. prolixus* and the end of a distal flagellomere. The arrows indicate the four recorded taste sensilla. Example of spike discharges of the GRNs housed in a taste sensillum. A typical firing response to 0.01 M Na is shown. Two salt-responsive GRNs were identified, S1-GRN and S2-GRN. As shown in the magnified area of the single-sensillum recording, S1-GRN showed action potentials of higher amplitude than S2-GRN.

(B and C) Occurrence of salt-sensitive GRNs in taste sensilla of the distal flagellomeres. Scatterplots, means ( $\pm$ SD), and fitted curves of spike frequencies versus logarithmic salt concentration of S1-GRN (B) and S2-GRN (C) are shown. S1-GRN responded to Na and K in a dose-dependent manner ( $R^2 = 0.94$  and  $0.95$ , respectively). S2-GRN only responded to Na

**Figure 2. Continued**

( $R^2 = 0.94$ ), but no dose-response relationship was detected to K ( $R^2 = 0$ ); 6 to 27 sensilla were tested for each salt concentration.

(D and E) Differing dynamics of the temporal pattern of GRNs responses. Peristimulus-time histogram of S1-GRN (D) and S2-GRN (E) in response to 0.01 M Na or K. Bars represent the number of action potentials recorded for each 100 ms bin. S1-GRN showed a phasic response profile, which was similar for both salts. In contrast, S2-GRN showed a tonic response pattern; 7 to 13 taste sensilla were tested.

(F and G) Amiloride blocks GRN responses to salts. Taste sensilla were treated with AMI (+AMI) or with distilled water (–AMI). Scatterplots are shown, and bars represent the mean spike frequency (mean  $\pm$  SEM) of S1-GRNs (F) and S2-GRN (G) in response to 0.01 and 0.2 M Na or K. The firing response of S1-GRN was significantly reduced by +AMI to both salts and concentrations. In contrast, the firing activity of S2-GRN was only blocked by +AMI at 0.01 M Na. Asterisks indicate statistical differences between +AMI and –AMI (Wilcoxon test,  $p < 0.03$ ) for each salt; 7 to 13 taste sensilla were tested per condition.

(H and I) Differing recovery time of GRN responses after amiloride blockade. Taste sensilla were treated with AMI as before (F–G). After +AMI application (0 min), and subsequently at 10-min intervals, the firing rate of GRNs was recorded. –AMI represents control of the response without AMI application. Scatterplots are shown, and bars represent the mean spike frequency (mean  $\pm$  SEM) of S1-GRN (H) and S2-GRN (I) in response to 0.01 M Na or K. The data at 0 min correspond to 0.01 M Na/K +AMI of (F) and (G). The recovery time of both GRNs is different. S1-GRN firing response recovered faster than S2-GRN. Asterisks indicate, for each salt, statistical differences between the –AMI and +AMI groups at each postapplication time (Wilcoxon test,  $k = 4$ ,  $\alpha' = 0.0125$ ,  $p < 0.002$ ). 7 to 8 taste sensilla were tested.

The –AMI insects consistently avoided feeding if exposed to high-Na/high-K membranes ( $p < 0.01$ ). However, +AMI-treated insects fed on high-Na/high-K-coated membranes. As expected, insects fed normally on no-Na/no-K membranes regardless of the treatment applied.

These results show that amiloride blocks the perception of high salt present on a feeding surface in *R. prolixus*.

**Intact antennae are required for high-salt feeding avoidance**

We asked, next, whether high-Na/high-K avoidance was triggered by antennal gustatory neurons. We hypothesized that ablation of the taste sensilla present on the tip of the distal flagellomeres would impede high-salt sensing on surfaces, as occurs for bitter substances (Pontes et al., 2014). Consequently, we expected that ablated insects would feed over a high-salt-coated membrane. To test this, the distal flagellomeres of both antennae were either cut (–ANT) or kept intact (+ANT). Then, we tested the feeding response to the AS of –ANT and +ANT groups, exposed to either a no-Na- or high-Na-coated membranes (Figure 1C).

As already shown, the presence of high-Na on the membrane prevented feeding on intact animals ( $p < 0.01$ ). Conversely, avoidance vanished when the distal flagellomeres were ablated. Note that cutting off the distal flagellomeres did not disturb insect feeding performance.

These results indicate that that high-Na on surfaces is detected by taste sensilla located on the distal antennal flagellomeres of *R. prolixus*.

**Two antennal GRNs detect salts**

Then, we examined the presence of salt-sensitive GRNs in the four taste sensilla of the distal antennal flagellomeres (Figure 2A). Single-sensillum taste recordings on these sensilla (shown in Figure 2A) revealed two salt-sensitive GRNs, S1-GRN and S2-GRN. Both GRNs were easily distinguished by the amplitude and waveform of their action potentials (Figure 2A). S1-GRN and S2-GRN increased their firing rate with salt concentration (Figures 2B and 2C). Although S1-GRN responded to Na and K in a dose-dependent manner ( $R^2 = 0.94$  and  $0.95$ , respectively), S2-GRN only responded to Na ( $R^2 = 0.94$ ), as revealed by the fit to a log-arithmic (dose) versus response curve, following a sigmoid shape. S2-GRN showed no dose-response relationship to K. In addition to the two salts tested, we checked whether S1- and S2-GRN also responded to another taste stimulus. Both neurons responded to the bitter alkaloid caffeine, although they showed different firing activity (Figure S2).

The temporal firing profiles of both neurons also showed notable differences. S1-GRN responded to Na/K phasically around its saturation limit (0.01 M, Figure 2D), turning to a phasic-tonic response at higher salt

concentrations (Figure S3A). The S2-GRN fired tonically upon Na stimulation (0.01 M, Figure 2E) with independence of its concentration (Figures 2E and S3B).

These results reveal that the four taste sensilla of the distal flagellomeres house at least two GRNs tuned either to Na and K or Na alone and that the salt receptors or transduction mechanisms of each GRN are different.

### Amiloride interferes with salt detection

Figure 1B showed that AMI blocks the perception of high-Na/high-K. Therefore, we expected that +AMI treatment would affect the firing activity of GRNs. To test this, taste sensilla were treated with +AMI, and subsequently, the response of both S1-GRN and S2-GRN to Na or K was recorded (Figures 2F–2I).

AMI blocked the activity of S1-GRN and S2-GRN by significantly decreasing their firing frequency to salts (Figures 2F and 2G). However, although the +AMI blocking effect on S1-GRN responses was independent of the Na/K concentration (Figure 2F,  $p < 0.01$ ), it only reduced S2-GRN responses at the lowest Na concentration tested (Figure 2G,  $p < 0.01$ ).

The recovery time of GRNs following +AMI application was also analyzed based on the response profiles (Figures 2H and 2I). The firing activity of S1-GRN to Na/K was significantly reduced immediately after AMI application (Figure 2H,  $p < 0.01$ ) and recovered 10 min later. A significant decreased response to Na following AMI exposure was also evident for S2-GRN (Figure 2I,  $p < 0.01$ ), which recovered after 20 min. However, when increasing the salt dose (0.2 M), the recovery time of S1-GRN was further delayed (*i.e.* 20 min), whereas no reduction was detected in the activity of S2-GRN along the 30 min of recordings (Figure S4).

These data show consistently that amiloride blocks salt detection in the GRNs of the antennae. They also show that the effect of AMI is markedly different in both neurons and dependent on the salt concentration.

### Antennal GRNs project into the ipsilateral antennal lobe

Next, we asked which were the neuropils involved in processing the information arising in the apical sensilla. Through anterograde mass fills we have previously shown that antennal (sensory) neurons innervate the antennal lobes (AL)—composed of glomerular structures as shown in the three-dimensional reconstruction—but also the antennal mechanosensory and motor centers (AMMC) and the subesophageal ganglion (SEZ) (Figures 3A and 3D) (Barrozo et al., 2009). Here, to trace the neurons housed in the four taste sensilla of the distal flagellomeres (Figure 2A), restricted backfills were carried out. For this purpose, we cut all four taste sensilla of the distal flagellomere of a single antenna and exposed them to the neuronal tracer (rhodamine). To assure that the neurons that became stained belong to these taste sensilla, we also exposed the contralateral antenna to the dye but kept the four taste sensilla intact. Seven preparations presented stained neuronal arborization in the glomeruli of the ipsilateral AL (Figure 3B). These arborizations were mainly found at glomeruli located in the anterior and ventral sides of the AL. This neuropil was the unique brain structure stained in all preparations. Besides, we never observed stained neurons arriving from the contralateral antennal nerve nor observed any kind of neuronal staining in the contralateral side of the brain.

In addition, to stain the neurons housed inside a single sensillum, stainings were also carried out by cutting and exposing a sole taste sensillum to another neuronal tracer (neurobiotin). Two preparations presented stained arborizations in the anterior and ventral AL glomeruli (Figure 3C). Figure 3E is an enlargement of the terminal arborizations of the stained neuron shown in 3C. Figure 3F is a reconstruction of the neuronal staining in 3E superimposed with the atlas of the AL (Figure 3D) of *R. prolixus*.

Thus, results of nine positive-stained confined backfills performed here consistently show that the axons of antennal GRNs arborize in glomeruli of the ipsilateral AL (Figures 3B, 3C, 3E, and 3F), indicating that the ALs are centers for the processing of antennal gustatory inputs.

### Two PPK salt receptor candidates

Next, we searched for salt receptor candidates in the genome of *R. prolixus*. We focused on PPKs because of their known role in salt sensing in insects (refs. above). The genome of *R. prolixus* revealed 10 PPK protein

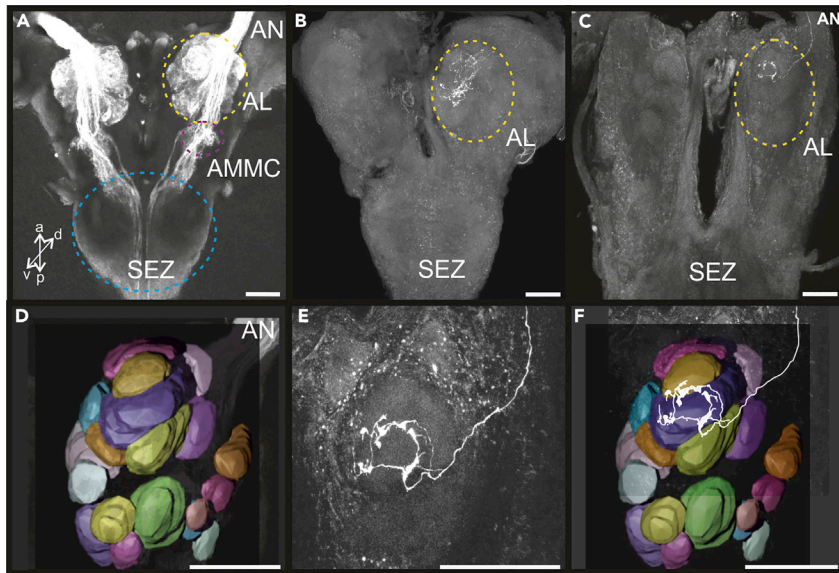


**Figure 3. Antennal GRNs project into the antennal lobes**

(A) Bilateral anterograde mass fills of the antennae revealing the brain structures innervated by antennal sensory neurons. The dashed lines delimit AL, AMMC, and SEZ.  
(B) Example of a confined backfill performed simultaneously in the four apical taste sensilla of the distal flagellomere with rhodamine. GRNs innervate the ipsilateral AL.  
(C) Example of a confined backfill performed in a single apical taste sensillum of the distal flagellomere with neurobiotin. Projections of one or more GRN/s arborize in the ipsilateral AL.  
(D) Three-dimensional atlas of the AL showing the glomeruli in different colors.  
(E) Enlargement of the AL showing the arborizations of the GRN/s stained in (C).  
(F) Three-dimensional atlas of the AL superimposed to the GRN/s stained in (C) and (E).  
AMMC, antennal mechanosensory and motor center; AL, antennal lobe; AN, antennal nerve; SEZ, subesophageal zone.  
Scale bar in A–F: 100  $\mu$ m.

sequences with a length between 337 and 564 amino acids (Latorre-Estivalis et al., 2017). These PPK protein sequences presented the amiloride-sensitive sodium domain (Latorre-estivalis et al., 2021). Among them, two PPKs were chosen as salt receptor candidates, the *RproPPK014276* (VectorBase RPRC014276) and the *RproPPK28* (VectorBase RPRC000471). The choice of these candidates was based on their clustering with *D. melanogaster* or *Ae. aegypti* PPK receptors (*DmelPPK19*, *DmelPPK28* and *AeagPPK301*) with a role in salt sensing or detection of hypo-osmotic solutions (Cameron et al., 2010; Chen et al., 2010; Liu et al., 2003; Matthews et al., 2019). *RproPPK014276* clustered with *DmelPPK19* and belongs to the PPK subfamily III. *RproPPK28* is orthologous of *DmelPPK28* and belongs to the PPK subfamily V (Latorre-estivalis et al., 2021). Besides, *RproPPK28* also clustered in the same clade with *AeagPPK301*.

Thus, we checked for the expression of *RproPPK014276* and *RproPPK28* in the distal antennal flagellomeres of *R. prolixus*. The RT-qPCR products found after 32–34 (*RproPPK014276*) and 29–32 threshold cycles (*RproPPK28*) confirmed their presence among the antennal transcripts (Figure 4A).

Based on these findings, *RproPPK014276* and *RproPPK28* were considered candidate salt receptors in *R. prolixus*.

### ***RproPPK014276* and *RproPPK28* genes can be knocked down**

Next, RNA interference experiments were carried out to study the role of *RproPPK014276* and *RproPPK28* in high-salt detection. Four experimental groups of insects were prepared: non-injected, dsRNA-ctrl (control group of dsRNA injection), dsRNA-*RproPPK014276*, and dsRNA-*RproPPK28*. Effective knockdown of transcript levels of *RproPPK014276* and *RproPPK28* was first assessed by RT-qPCR (Figures 4B and 4C).

A significant reduction of transcript levels for *RproPPK014276* (Figure 4B,  $p < 0.001$ ) and *RproPPK28* (Figure 4C,  $p < 0.001$ ) was well established with respect to non-injected and dsRNA-ctrl groups ( $p < 0.05$ ).

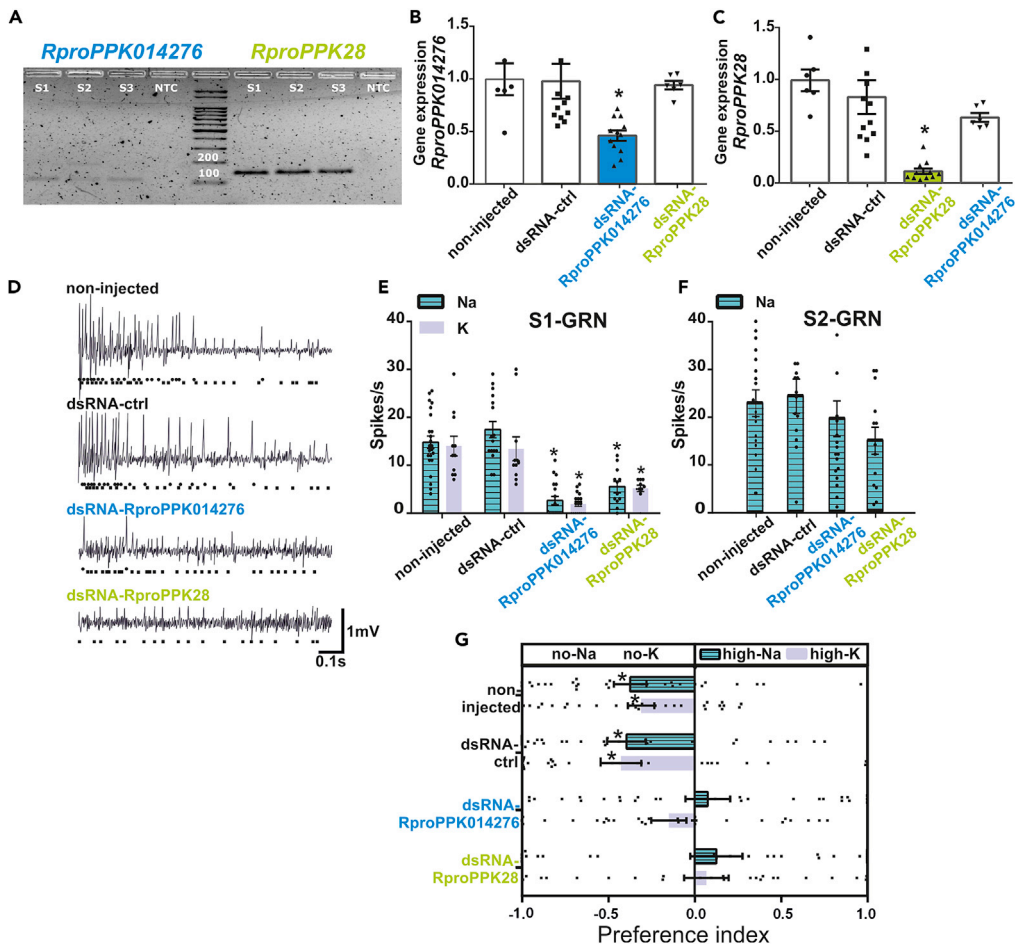


**Figure 4. High-salt avoidance depends on *RproPPK014276* and *RproPPK28*, the functional salt receptors of S1-GRN**

(A) *RproPPK014276* and *RproPPK28* are expressed in the distal antennal flagellomeres. Electrophoresis of qPCR products of three replicates (S1, S2, S3) and a nontemplate control (NTC). *RproPPK014276* and *RproPPK28* qPCR products were detected after threshold cycles of 32–34 and 29–32, respectively, confirming their expression in the antenna.

(B and C) Transcript levels of *RproPPK014276* and *RproPPK28* decay following RNAi. Scatterplots are shown, and bars represent the relative transcript levels (mean  $\pm$  SEM) of *RproPPK014276* (B) and *RproPPK28* (C) in noninjected and dsRNA-injected groups. The expression levels of *RproPPK014276* and *RproPPK28* decayed significantly only when the corresponding dsRNA was injected. Selective knockdown of the gene of interest was also confirmed, as the dsRNA-*RproPPK28* group showed similar transcript levels for the *RproPPK014276* gene as those observed in control groups (B, last bar). Similarly, the dsRNA-*RproPPK014276* group showed similar transcript levels for *RproPPK28* as did the control groups (C, last bar). Asterisks denote significant differences across groups (Kruskal-Wallis test, Dunn's *post hoc* comparisons,  $p < 0.001$ ); 6 to 12 replicates were carried out per treatment.

(D and F) *RproPPKs* knockdown negatively affects salt detection. Raw traces from recordings of GRNs (D) of noninjected and dsRNA-injected groups in response to 0.01 M Na. Diamonds and squares below traces represent the spikes of S1-GRN and S2-GRN, respectively, following spike sorting. Spike frequencies of S1-GRN (E) and S2-GRN (F) in response to 0.01 M Na or K in noninjected and dsRNA-injected groups. Scatterplots are shown, and bars represent the mean spike frequency for each condition (mean  $\pm$  SEM). Both *RproPPK014276* and *RproPPK28* are required for proper S1-GRN response to Na or K. In contrast, *RproPPKs* silencing did not affect the responses of S2-GRN to Na. Asterisks denote, for each salt, statistical differences between noninjected and dsRNA-injected groups (Kruskal-Wallis test, Dunn's *post hoc* comparisons,  $p < 0.0001$ ); 10 to 23 sensilla were tested.

(G) Loss of high-salt avoidance after *RproPPKs* silencing. Preference of bugs was tested in a simultaneous two-choice arena, one-half zone coated with high-Na/high-K (1 M) and the other with no-Na/no-K (0 M, distilled water). Scatterplots are shown, and bars represent the mean preference index (PI) (mean  $\pm$  SEM), 0 denoting equal time spent within each zone and  $-1$  and  $1$  denoting avoidance or preference for the high-Na/high-K zone, respectively. Noninjected and dsRNA-ctrl groups avoided high-Na/high-K-coated substrates. dsRNA-*RproPPK014276* and dsRNA-*RproPPK28* groups showed no preference for any zone of the arena. Asterisks denote, for each salt, statistical differences between the PI and 0 for each experimental group (t test,  $p < 0.001$ ); 24 to 28 replicates were carried out for each experimental condition.

Furthermore, we checked that gene knockdown was specifically targeted to the mRNA of interest in each dsRNA group. For this, we checked whether the expression of *RproPPK28* was not affected when knocking down *RproPPK014276* and vice versa, as shown in [Figures 4B and 4C](#) (last bars).

### Knockdown of *RproPPK014276* or *RproPPK28* abolishes salt detection only in S1-GRN

Then, we examined whether knockdown of *RproPPK014276* and *RproPPK28* altered the response of S1-GRN and S2-GRN to salts. Consequently, the firing activity of S1-GRN and S2-GRN was examined on the four taste sensilla ([Figure 2A](#)) of non-injected and dsRNA-injected insects ([Figures 4D–4F](#)).

Raw traces from GRN recordings of non-injected and dsRNA-injected groups are shown in [Figure 4D](#), and action potentials of GRNs are quantified in [Figures 4E and 4F](#). The spike frequency of S1-GRN to Na or K was significantly decreased ([Figure 4E](#),  $p < 0.0001$ ) in dsRNA-*RproPPK014276* and in dsRNA-*RproPPK28* groups with respect to non-injected and dsRNA-ctrl ones ( $p < 0.05$ ). In contrast, the firing frequency of S2-GRN to Na showed no significant difference across groups ([Figure 4F](#)).

These results show that *RproPPK014276* and *RproPPK28* participate in salt detection in S1-GRN. Furthermore, the results reveal that a decreased expression of either of these genes suppresses the response to Na or K, demonstrating that both PPKs are necessary for S1-GRN to detect salts.

### *RproPPK014276* and *RproPPK28* are responsible for high-salt avoidance

Next, we examined whether *RproPPK014276* and *RproPPK28* were involved in the avoidance of high-salt substrates. *R. prolixus* avoid high-Na/high-K substrates if an alternative clean substrate choice is available ([Masagué et al., 2020](#)). Therefore, we tested the preference of knocked down and control insects for substrates coated with high-Na/high-K versus no-Na/no-K in a two-choice arena ([Figure 4G](#)).

As expected, non-injected and dsRNA-ctrl insects avoided the high-Na/high-K zone of the two-choice arena (non-injected,  $p < 0.001$ ; dsRNA-ctrl,  $p < 0.005$ ). In contrast, dsRNA-*RproPPK014276*- and dsRNA-*RproPPK28*-injected insects showed no significant preference for a zone of the arena, i.e., they lost their avoidance of the high-Na/high-K zone.

These results show that reduced levels of *RproPPK014276* or *RproPPK28* prevent high-Na/high-K sensing and therefore high-salt avoidance. Furthermore, the expression of both genes is necessary to signal the presence of high salt and, ultimately, to trigger the behavioral avoidance of high-salt substrates.

## DISCUSSION

Innate avoidance is triggered when a threat is detected through interaction with deterrent sensory inputs. Our study reveals the molecular and physiological basis of high-salt taste detection in a blood-sucking insect of great epidemiological interest. We characterized the behavioral response of *R. prolixus* to high salt and identified the sensory organs, chemosensory neurons, and molecular taste receptors mediating high-salt detection. Besides, we uncovered the downstream brain regions for antennal taste processing.

### High-salt detection prevents feeding and triggers avoidance responses

*R. prolixus* performs a gustatory evaluation of the food and walking substrates before making appropriate decisions. Here, we show that high-salt detection on the bite membrane negatively interferes with biting and feeding decisions in *R. prolixus*. Indeed, high-salt doses generally hold a negative valence, as seen in rodents and *D. melanogaster* ([Chandrashekar et al., 2010](#); [Liu et al., 2003](#); [Niewalda et al., 2008](#); [Oka et al., 2013](#)). It is important to mention that low-salt-coated membranes, i.e. 0.15 M, corresponding to the upper limit of sodium levels found in human sweat (ca. 0.01–0.17 M, as referred to in [Baker and Wolfe, 2020](#); [Buono et al., 2007](#); and [Cage and Dobson, 1965](#)), neither enhance nor prevent feeding when compared with a salt-free membrane. Under these conditions, i.e. no-salt or low-salt, the heat emitted by the feeder is sufficient to trigger similar biting and feeding performances in *R. prolixus*, suggesting that low-salt detection has no evident behavioral role in the feeding context. Interestingly, the physiological mechanisms behind high-salt perception and low-salt perception have been shown to be different ([Chandrashekar et al., 2010](#); [Jaeger et al., 2018](#); [Zhang et al., 2013](#)).

In rodents and *D. melanogaster*, the tongue and the proboscis are the main taste organs involved in salt sensing during feeding. In *R. prolixus*, detection of high-salt content on the bite site begins at the antenna level as we have shown. In absence of the antennal flagellomeres, feeding avoidance of kissing bugs on high-salt substrates vanished. Likewise, feeding inhibition triggered by the detection of bitter compounds in *R. prolixus* was reverted when the distal ends of both antennae were absent (Pontes et al., 2014). Nevertheless, it cannot be ruled out that other taste sensilla present, for example on the tarsi, can also detect gustatory stimuli (Barrozo et al., 2017). However, the antennae appear to be key taste organs to signal the presence of negative inputs during bite site evaluation in *R. prolixus* (Pontes et al., 2014, this work). Thereby, the antennae, which never get in contact with blood, assess exclusively external cues, tasting and exploring, for example, the host skin or the walking substrate. Besides the role of the antennae in the feeding context, we show the predictive character of the taste system has for a blood-sucking insect whose decision to feed on a highly appetitive solution is hampered by the detection of high-salt content at the bite site.

### Antennal GRNs involved in salt detection

Two GRNs, housed in the taste sensilla of the distal flagellomeres of *R. prolixus*, are responsible for antennal salt detection. Although both were activated by Na, only S1-GRN was also sensitive to K. Interestingly, through discriminative learning protocols, in a previous study we showed that *R. prolixus* cannot discriminate Na from K (Masagué et al., 2020). The detection of both cations through the same S1-GRN could explain this lack of discrimination between Na and K.

S1-GRN and S2-GRN showed clear physiological differences in the temporal firing patterns in response to salts. Although S1-GRN showed phasic to phasic-tonic responses, S2-GRN exhibited tonic responses. The phasic component of the response of receptor neurons may provide significant information about stimulus intensity and quality (Bruyne et al., 2001; Hallem and Carlson, 2006). Besides, a defined peak of impulse frequency enables the animal to recognize the onset of stimulation (Kaissling et al., 1987). The existence and relevance of a spatiotemporal code across GRNs, likely signaling the quality and intensity of the taste stimulus, has been shown by several studies (Dethier and Crnjar, 1982; Glendinning et al., 2006; Miriyala et al., 2018; Reiter et al., 2015). Thus, S1-GRN could quickly warn the insect about the presence of a noxious salty stimulus, whereas a tonic response such as in S2-GRN could indicate its persistence.

S1-GRN and S2-GRN were sensitive to amiloride blockade, although effects were different for each neuron type. These findings demonstrated the existence of at least two different amiloride-sensitive salt receptors in each GRN. Furthermore, the different specificity of S1-GRN and S2-GRN for Na/K or Na only, respectively, also confirms the presence of different salt receptors in both neurons. Looking at the response of S1-GRN to the highest dose of salt tested allows us to infer a noncompetitive blockade by amiloride, as amiloride still blocked the responses of S1-GRN but not S2-GRN. These findings suggest that in insects treated with amiloride (Figure 1B) the S2-GRN was active but not able to trigger high-salt avoidance. But the amiloride blockade of S1-GRN resulted in the loss of high-salt responsiveness and consequently favored *R. prolixus* to feed on a high-salt bite site. Similarly, avoidance of high-salt substrates disappeared when kissing bugs were treated with amiloride, and their preference was evaluated in a dual-choice arena between high-salt versus no-salt substrates (Masagué et al., 2020).

### Two PPKs are required for high-salt taste

*RproPPK014276* and *RproPPK28* and eight other PPK genes are expressed in the antennae of *R. prolixus* (Latorre-Estivalis et al., 2017). In addition, *RproPPK014276* and *RproPPK28* are expressed in the CNS of *R. prolixus*, showing levels close to those found in the antennae according to transcriptomic data available in VectorBase. Besides, this database also reports that *RproPPK28* is highly expressed in the testes, whereas no expression was detected in other tissues such as ovaries, Malpighian tubules, fat body, and gut. Yet, the functional role of PPKs in hematophagous insects had not been studied until recently (Mathews et al., 2019 and this work). As a first approach, we focused on *RproPPK014276* and *RproPPK28* because they clustered with *DmelPPK19* and *DmelPPK28* and *AaegPPK301*. Notably, *DmelPPK19* has been related to ion detection (Liu et al., 2003). Following disruption of *DmelPPK19*, flies failed to recognize low Na or K concentrations. *DmelPPK28* was associated instead with the detection of hypo-osmotic solutions in flies (Cameron et al., 2010; Chen et al., 2010). Recently, *AaegPPK301* was found to be sensitive to water and low salt and required for the initiation of egg laying by females of the mosquito *Ae. aegypti* (Mathews et al., 2019). *DmelPPK19* has also been related to high-salt detection in *D. melanogaster* (Liu et al.,

2003). As predicted for known DEG/ENaC and PPKs sequences, it was shown that *R. prolixus* PPKs present two transmembrane domains, a cysteine-rich domain and a Deg motif, and revealed the presence of an amiloride-binding domain next to the pore region (Latorre-estivalis et al., 2021). But even more importantly, we showed that following *RproPPK014276* and *RproPPK28* knockdown, avoidance of high-Na/high-K substrates in *R. prolixus* was abolished. Notably, to generate high-salt avoidance, the inactivation of a single PPK was enough to disrupt the neuronal and behavioral responsiveness to high salt. Indeed, Ben-Shahar (2011) proposed that PPKs form homo- or heteromeric protein complexes of three subunits (or multiples of three) to generate cation channels. We suggest that these two *RproPPK* receptors likely form a heteromultimeric complex as those of other PPKs and ENaC receptors (Kellenberger and Schild, 2002), as is the case for low-salt sensing (mediated by *DmelPPK11-DmelPPK19*) (Liu et al., 2003) and nociceptive mechanosensation (mediated by *Dmelppk1-Dmelppk26*) (Zelle et al., 2013); this could explain the differing roles of *PPK28* in *R. prolixus* and *D. melanogaster* besides the evolutionary distance between these two species.

### One GRN and two PPKs are responsible for high-salt avoidance

Knocking down the expression of either *RproPPK014276* or *RproPPK28* induced an abrupt decay of S1-GRN firing responses to Na and K. As a consequence, insects showed a random behavior on the two-choice preference arena, losing avoidance for a high-salt substrate. However, the response of S2-GRN to Na was not affected by PPKs silencing, indicating that S2-GRNs, as shown before for amiloride experiments, express a different type/s of salt receptor/s compared with S1-GRN. Different salt receptors, other than PPKs, are involved in salt sensing in *D. melanogaster*, for example, *IR76b*, *IR94e*, and *sano* (see refs. above). Besides, more than one neuron are sensitive to salts in all animals studied so far (Chandrashekar et al., 2010; Jaeger et al., 2018; Liu et al., 2003; Meunier et al., 2003; Oka et al., 2013; Spector et al., 1996). For example, two salt-sensitive GRNs (i.e. GR66a-GRNs and PPK23-GRNs) have been associated with high-salt detection by *D. melanogaster*. These high-salt sensing GRNs of fruit flies showed to be ion nonselective, in contrast to the low-salt sensing GRN (i.e. GR64f-GRN), which was specifically tuned to NaCl. Here, we show that S1-GRN activation, through the expression of *RproPPK014276* and *RproPPK28*, provides kissing bugs with useful information about the aversive saltiness of a substrate. Future studies in *R. prolixus* will unveil if there are other chemosensory receptors involved in salt detection too.

### Antennal gustatory inputs are processed in the ALs

Antennal receptor neurons send their axons via the antennal nerves to the deutocerebrum, which is composed of two parts: the antennal lobe (AL) and the antennal mechanosensory and motor center (AMMC) (Homborg et al., 1989). The ALs are the primary processing centers that receive all inputs conveying olfactory information gathered by the antennae (Hansson and Anton, 2000) but also integrate inputs from other sensory modalities such as thermo-, hygro-, and mechano-reception (Nishino et al., 2003; Zeiner and Tichy, 1998, 2000). Through mass backfills of the antennae of *R. prolixus*, we have previously shown that sensory neurons project to the ALs, the AMMC, the subesophageal (SEZ), prothoracic, and posterior ganglia (Barrozo et al., 2009). Here we have found that GRNs of the taste sensilla at the distal flagellomere target exclusively the ALs. Hitherto, the brain processing center for gustatory information had been attributed to the SEZ (Mitchell et al., 1999), receiving inputs mainly from mouthpart sensilla but also GRNs present in legs and antennae (Kvello et al., 2010; Scott, 2018). For example, antennal GRNs in moths and bees project directly to the SEZ and the AMMC (Haupt, 2007; Jørgensen et al., 2006; Kvello et al., 2010; Nishino et al., 2005; Popescu et al., 2013). However, the SEZ also receives axons from olfactory receptor neurons of the proboscis labellum in the mosquito *Anopheles gambiae* (Riabinina et al., 2016). Even if the SEZ and ALs are known as gustatory and olfactory centers, respectively, our results (this work) and those of Riabinina et al. (2016) indicate that these neuropils should not be considered exclusively dedicated to a single chemosensory modality. Considering that different sensory modalities reach the ALs (e.g. olfactory, heat, humidity, mechanosensory, and gustatory), this neuropile should indeed be considered as a multimodal brain processing center of antennal information in insects. Therefore, the hypothesis that ALs act as multimodal integration centers deserves to be further investigated. Future functional studies on the AL will provide direct evidence on its role as a gustatory processing center.

### Final remarks

Compounds triggering aversive responses, eliciting avoidance of inedible food, or preventing oviposition are considered deterrents (Debboun et al., 2015). Those that reduce the rate of biting of blood-feeding insects are of particular interest due to the inherent risk of disease transmission posed by each bite. Knowing

that the taste sense drives stereotypical rejection responses may allow finding gustatory deterrents for disease vectors complementing known repellent volatiles.

### Limitations of the study

Our results revealed the presence of GRNs projecting to ALs; however, the success rate using single sensillum staining was limited. Therefore, to improve staining efficiency, we performed massive backfills of the four taste sensilla of the distal flagellomere. On the other hand, it is not possible to know if the stained neuron/s is/are neuron/s sensitive to salt or not. Only physiological studies will certainly provide corroborating evidence that salt processing takes place in ALs.

### STAR★METHODS

Detailed methods are provided in the online version of this paper and include the following:

- KEY RESOURCES TABLE
- RESOURCE AVAILABILITY
  - Lead contact
  - Materials availability
  - Data and code availability
- EXPERIMENTAL MODEL AND SUBJECT DETAILS
  - Insects
- METHODS DETAILS
  - Feeding assays
  - Electrophysiological recordings
  - Tracing of GRNs
  - Antennal expression of PPKs
  - RNA interference
- QUANTIFICATION AND STATISTICAL ANALYSIS
  - Feeding assays
  - Electrophysiological recordings
  - Gene expression
  - Two-choice behavioral assays

### SUPPLEMENTAL INFORMATION

Supplemental information can be found online at <https://doi.org/10.1016/j.isci.2022.104502>.

### ACKNOWLEDGMENTS

We thank Sheila Ons for providing equipment and PCR reagents. We deeply thank Sylvia Anton, Carolina Reisenman, Meghan Laturney, Sharon Hill, Rickard Ignell, and Anupama Dahanukar and lab members for fruitful suggestions that improved the manuscript. The financial support was provided by ANPCyT (Préstamo BID PICT2013-1253, Préstamo BID PICT2019-0257 to RBB, Préstamo BID PICT2015-2825 to GP and Préstamo BID PICT2016-3103 to JMLE). MGL thanks FIOCRUZ, INCTEM (Project: 465678/2014-9), and CNPq (Project: 311826/2019-9).

### AUTHOR CONTRIBUTIONS

RBB designed research; GP, JMLE, MLG, AC, MBA, and RBB performed research; GP, JMLE, MGL, MBA, and RBB contributed with reagents or analytic tools; GP, JMLE, MLG, MBA, and RBB analyzed data; GP, JMLE, MLG, AC, MBA, MGL, and RBB wrote the paper.

### DECLARATION OF INTERESTS

The authors declare no conflict of interests.

Received: January 24, 2022

Revised: April 14, 2022

Accepted: May 26, 2022

Published: July 15, 2022

## REFERENCES

- Alves, G., Sallé, J., Chaudy, S., Dupas, S., and Manière, G. (2014). High-NaCl perception in *Drosophila melanogaster*. *J. Neurosci.* 34, 10884–10891. <https://doi.org/10.1523/jneurosci.4795-13.2014>.
- Baker, L.B., and Wolfe, A.S. (2020). Physiological mechanisms determining eccrine sweat composition. *Eur. J. Appl. Physiol.* 120, 719–752. <https://doi.org/10.1007/s00421-020-04323-7>.
- Barrozo, R.B. (2019). Food recognition in hematophagous insects. *Curr. Opin. Insect Sci.* 34, 55–60. <https://doi.org/10.1016/j.cois.2019.03.001>.
- Barrozo, R.B., Minoli, S.A., and Lazzari, C.R. (2004). Circadian rhythm of behavioural responsiveness to carbon dioxide in the blood-sucking bug *Triatoma infestans* (Heteroptera: Reduviidae). *J. Insect Physiol.* 50, 249–254. <https://doi.org/10.1016/j.jinsphys.2004.01.001>.
- Barrozo, R.B., Couton, L., Lazzari, C.R., Insausti, T.C., Minoli, S.A., Fresquet, N., Rospars, J.-P., and Anton, S. (2009). Antennal pathways in the central nervous system of a blood-sucking bug, *Rhodnius prolixus*. *Arthropod. Struct. Dev.* 38, 101–110. <https://doi.org/10.1016/j.asd.2008.08.004>.
- Barrozo, R.B., Reizenman, C.E., Guerenstein, P., Lazzari, C.R., and Lorenzo, M.G. (2017). An inside look at the sensory biology of triatomines. *J. Insect Physiol.* 97, 3–19. <https://doi.org/10.1016/j.jinsphys.2016.11.003>.
- Ben-Shahar, Y. (2011). Sensory functions for degenerin/epithelial sodium channels (DEG/ENaC). *Adv. Genet.* 76, 2–26.
- Bodin, A., Barrozo, R.B., Couton, L., and Lazzari, C.R. (2008). Temporal modulation and adaptive control of the behavioural response to odours in *Rhodnius prolixus*. *J. Insect Physiol.* 54, 1343–1348. <https://doi.org/10.1016/j.jinsphys.2008.07.004>.
- Bruyne, M.D., Foster, K., Carlson, J.R., Haven, N., and de Bruyne, M. (2001). Odor coding in the *Drosophila* antenna. *Neuron* 30, 537–552. [https://doi.org/10.1016/s0896-6273\(01\)00289-6](https://doi.org/10.1016/s0896-6273(01)00289-6).
- Buono, M.J., Ball, K.D., and Kolkhorst, F.W. (2007). Sodium ion concentration vs. sweat rate relationship in humans. *J. Appl. Physiol.* 103, 990–994. <https://doi.org/10.1152/jappphysiol.00015.2007>.
- Cage, G.W., and Dobson, R.L. (1965). Sodium secretion and reabsorption in the human eccrine sweat gland. *J. Clin. Invest.* 44, 1270–1276. <https://doi.org/10.1172/jci105233>.
- Cameron, P., Hiroi, M., Ngai, J., and Scott, K. (2010). The molecular basis for water taste in *Drosophila*. *Nature* 465, 91–95. <https://doi.org/10.1038/nature09011>.
- Cano, A., Pontes, G., Sfara, V., Anfossi, D., and Barrozo, R.B. (2017). Nitric oxide contributes to high-salt perception in a blood-sucking insect model. *Sci. Rep.* 7, 15551. <https://doi.org/10.1038/s41598-017-15861-0>.
- Chandrashekar, J., Kuhn, C., Oka, Y., Yarmolinsky, D.A., Hummler, E., Ryba, N.J.P., and Zuker, C.S. (2010). The cells and peripheral representation of sodium taste in mice. *Nature* 464, 297–301. <https://doi.org/10.1038/nature08783>.
- Chapman, R.F. (2003). Contact chemoreception in feeding by phytophagous insects. *Annu. Rev. Entomol.* 48, 455–484. <https://doi.org/10.1146/annurev.ento.48.091801.112629>.
- Chen, Z., Wang, Q., and Wang, Z. (2010). The amiloride-sensitive epithelial Na<sup>+</sup> channel PPK28 is essential for *Drosophila* gustatory water reception. *J. Neurosci.* 30, 6247–6252. <https://doi.org/10.1523/jneurosci.0627-10.2010>.
- Debboun, M., Frances, S.P., and Strickman, D.A. (2015). *Insect repellents handbook*. In *Insect Repellents Handbook*, M. Debboun, S.P. Frances, and D.A. Strickman, eds. (Boca Raton: CRC Press, Taylor & Francis Group), p. 400.
- Dethier, V.G., and Crnjar, R.M. (1982). Candidate codes in the gustatory system of caterpillars. *J. Gen. Physiol.* 79, 549–569. <https://doi.org/10.1085/jgp.79.4.549>.
- Edwards, M.S., Stimpert, K.K., and Montgomery, S.P. (2017). Addressing the challenges of Chagas disease an emerging health concern in the United States. *Infect. Dis. Clin. Pract.* 25, 118–125. <https://doi.org/10.1097/ipc.0000000000000512>.
- Flores, G.B., and Lazzari, C.R. (1996). The role of the antennae in *Triatoma infestans*: orientation towards thermal sources. *J. Insect Physiol.* 42, 433–440. [https://doi.org/10.1016/0022-1910\(95\)00137-9](https://doi.org/10.1016/0022-1910(95)00137-9).
- Freeman, E.G., and Dahanukar, A. (2015). Molecular neurobiology of *Drosophila* taste. *Curr. Opin. Neurobiol.* 34, 140–148. <https://doi.org/10.1016/j.conb.2015.06.001>.
- Friend, W.G., and Smith, J.J.B. (1977). Factors affecting feeding by bloodsucking insects. *Annu. Rev. Entomol.* 22, 309–331. <https://doi.org/10.1146/annurev.en.22.010177.001521>.
- Glendinning, J.I., Davis, A., and Rai, M. (2006). Temporal coding mediates discrimination of “bitter” taste stimuli by an insect. *J. Neurosci.* 26, 8900–8908. <https://doi.org/10.1523/jneurosci.2351-06.2006>.
- Guerenstein, P.G., and Núñez, J. (1994). Feeding response of the haematophagous bugs *Rhodnius prolixus* and *Triatoma infestans* to saline solutions: a comparative study. *J. Insect Physiol.* 40, 747–752. [https://doi.org/10.1016/0022-1910\(94\)90002-7](https://doi.org/10.1016/0022-1910(94)90002-7).
- Hallen, E.A., and Carlson, J.R. (2006). Coding of odors by a receptor repertoire. *Cell* 125, 143–160. <https://doi.org/10.1016/j.cell.2006.01.050>.
- Halpern, B.P. (1998). Amiloride and vertebrate gustatory responses to NaCl. *Neurosci. Biobehav. Rev.* 23, 5–47. [https://doi.org/10.1016/s0149-7634\(97\)00063-8](https://doi.org/10.1016/s0149-7634(97)00063-8).
- Hansson, B.S., and Anton, S. (2000). Function and morphology of the antennal lobe: new Developments. *Annu. Rev. Entomol.* 45, 203–231. <https://doi.org/10.1146/annurev.ento.45.1.203>.
- Haupt, S.S. (2007). Central gustatory projections and side-specificity of operant antennal muscle conditioning in the honeybee. *J. Comp. Physiol.* A Neuroethol. Sensory, Neural, Behav. Physiol. 193, 523–535. <https://doi.org/10.1007/s00359-007-0208-z>.
- Hiroi, M., Meunier, N., Marion-Poll, F., and Tanimura, T. (2004). Two antagonistic gustatory receptor neurons responding to sweet-salty and bitter taste in *Drosophila*. *J. Neurobiol.* 61, 333–342. <https://doi.org/10.1002/neu.20063>.
- Hodgson, E.S., Lettvin, J.Y., and Roeder, K.D. (1955). Physiology of a primary chemoreceptor unit. *Science* 122, 417–418. <https://doi.org/10.1126/science.122.3166.417-a>.
- Homberg, U., Christensen, T.A., Hildebrand, J.G., and Homberg, U. (1989). Structure and function of the deutocerebrum in insects. *Annu. Rev. Entomol.* 34, 477–501. <https://doi.org/10.1146/annurev.en.34.010189.002401>.
- Jaeger, A.H., Stanley, M., Weiss, Z.F., Musso, P.Y., Chan, R.C.W., Zhang, H., Feldman-Kiss, D., and Gordon, M.D. (2018). A complex peripheral code for salt taste in *Drosophila*. *Elife* 7, e37167. <https://doi.org/10.7554/elif37167>.
- Jenkins, J.B., and Tompkins, L. (1990). Effects of amiloride on taste responses of *Drosophila melanogaster* adults and larvae. *J. Insect Physiol.* 36, 613–618. [https://doi.org/10.1016/0022-1910\(90\)90064-m](https://doi.org/10.1016/0022-1910(90)90064-m).
- Jørgensen, K., Kvello, P., Almaas, T.J., and Mustaparta, H. (2006). Two closely located areas in the subesophageal ganglion and the tritocerebrum receive projections of gustatory receptor neurons located on the antennae and the proboscis in the moth *Heliothis virescens*. *J. Comp. Neurol.* 496, 121–134. <https://doi.org/10.1002/cne.20908>.
- Kaisling, K.-E., Strausfeld, C.Z., and Rumbo, E.R. (1987). Adaptation processes in insect olfactory receptors. Mechanisms and behavioral significance. *Ann. N. Y. Acad. Sci.* 510, 104–112. <https://doi.org/10.1111/j.1749-6632.1987.tb43475.x>.
- Kellenberger, S., and Schild, L. (2002). Epithelial sodium channel/degenerin family of ion channels: a variety of functions for a shared structure. *Physiol. Rev.* 82, 735–767. <https://doi.org/10.1152/physrev.00007.2002>.
- Kvello, P., Jørgensen, K., and Mustaparta, H. (2010). Central gustatory neurons integrate taste quality information from four appendages in the moth *Heliothis virescens*. *J. Neurophysiol.* 103, 2965–2981. <https://doi.org/10.1152/jn.00985.2009>.
- Latorre-estivalis, J.M., Almeida, F.C., Pontes, G., Dopazo, H., Lorenzo, M.G., and Lorenzo, M.G. (2021). Evolution of the insect PPK gene family. *Genome Biol. Evol.* 13, evab185. <https://doi.org/10.1093/gbe/evab185>.
- Latorre-Estivalis, J.M., Robertson, H.M., Walden, K.K.O., Ruiz, J., Gonçalves, L.O., Guarneri, A.A., and Lorenzo, M.G. (2017). The molecular sensory machinery of a Chagas disease vector: expression changes through imaginal moult and sexually dimorphic features. *Sci. Rep.* 7, 40049. <https://doi.org/10.1038/srep40049>.

- Lee, M.J., Sung, H.Y., Jo, H., Kim, H.W., Choi, M.S., Kwon, J.Y., and Kang, K. (2017). Ionotropic receptor 76b is required for gustatory aversion to excessive Na<sup>+</sup> in *Drosophila*. *Mol. Cells* 40, 787–795. <https://doi.org/10.14348/molcells.2017.0160>.
- Liman, E.R., Zhang, Y.V., and Montell, C. (2014). Peripheral coding of taste. *Neuron* 81, 984–1000. <https://doi.org/10.1016/j.neuron.2014.02.022>.
- Liu, L., Leonard, A.S., Motto, D.G., Feller, M.A., Price, M.P., Johnson, W.A., and Welsh, M.J. (2003). Contribution of *Drosophila* DEG/ENaC genes to salt taste. *Neuron* 39, 133–146. [https://doi.org/10.1016/s0896-6273\(03\)00394-5](https://doi.org/10.1016/s0896-6273(03)00394-5).
- Marion-Poll, F. (1996). Display and analysis of electrophysiological data under Windows™. *Entomol. Exp. Appl.* 80, 116–119. <https://doi.org/10.1111/j.1570-7458.1996.tb00900.x>.
- Masagué, S., Cano, A., Asparch, Y., Barrozo, R.B., and Minoli, S. (2020). Sensory discrimination between aversive salty and bitter tastes in a hematophagous insect. *Eur. J. Neurosci.* 51, 1867–1880. <https://doi.org/10.1111/ejn.14702>.
- Matthews, B.J., Younger, M.A., and Vosshall, L.B. (2019). The ion channel ppk301 controls freshwater egg-laying in the mosquito *Aedes aegypti*. *Elife* 8, e43963. <https://doi.org/10.7554/eLife.43963>.
- Meunier, N., Marion-Poll, F., Rospars, J.-P., and Tanimura, T. (2003). Peripheral coding of bitter taste in *Drosophila*. *J. Neurobiol.* 56, 139–152. <https://doi.org/10.1002/neu.10235>.
- Minoli, S., Cano, A., Pontes, G., Magallanes, A., Roldán, N., and Barrozo, R.B. (2018). Learning spatial aversion is sensory-specific in the hematophagous insect *Rhodnius prolixus*. *Front. Psychol.* 9, 989. <https://doi.org/10.3389/fpsyg.2018.00989>.
- Miriyala, A., Kessler, S., Rind, F.C., and Wright, G.A. (2018). Burst firing in bee gustatory neurons prevents adaptation. *Curr. Biol.* 28, 1585–1594.e3. <https://doi.org/10.1016/j.cub.2018.03.070>.
- Mitchell, B.K., Itagaki, H., and Rivet, M.P. (1999). Peripheral and central structures involved in insect gustation. *Microsc. Res. Tech.* 47, 401–415. [https://doi.org/10.1002/\(sici\)1097-0029\(19991215\)47:6<401::aid-jemt4>3.0.co;2-7](https://doi.org/10.1002/(sici)1097-0029(19991215)47:6<401::aid-jemt4>3.0.co;2-7).
- Muñoz, I.J., Schilman, P.E., and Barrozo, R.B. (2020). Impact of alkaloids in food consumption, metabolism and survival in a blood-sucking insect. *Sci. Rep.* 10, 9443. <https://doi.org/10.1038/s41598-020-65932-y>.
- Mutebi, J.-P., Hawley, W.A., and Brogdon, W.G. (2017). Protection against Mosquitoes, Ticks, & Other Arthropods - Chapter 2 - 2018 (Yellow Book, Travelers' Health, CDC).
- Newland, P.L., and Yates, P. (2008). Nitric oxide modulates salt and sugar responses via different signaling pathways. *Chem. Senses* 33, 347–356. <https://doi.org/10.1093/chemse/bjm094>.
- Niewalda, T., Singhal, N., Fiala, A., Saumweber, T., Wegener, S., and Gerber, B. (2008). Salt processing in larval *Drosophila*: choice, feeding, and learning shift from appetitive to aversive in a concentration-dependent way. *Chem. Senses* 33, 685–692. <https://doi.org/10.1093/chemse/bjn037>.
- Nishino, H., Yamashita, S., Yamazaki, Y., Nishikawa, M., Yokohari, F., and Mizunami, M. (2003). Projection neurons originating from thermo- and hyposensory glomeruli in the antennal lobe of the cockroach. *J. Comp. Neurol.* 455, 40–55. <https://doi.org/10.1002/cne.10450>.
- Nishino, H., Nishikawa, M., Yokohari, F., and Mizunami, M. (2005). Dual, multilayered somatosensory maps formed by antennal tactile and contact chemosensory afferents in an insect brain. *J. Comp. Neurol.* 493, 291–308. <https://doi.org/10.1002/cne.20757>.
- Oka, Y., Butnaru, M., von Buchholtz, L., Ryba, N.J.P., and Zuker, C.S. (2013). High salt recruits aversive taste pathways. *Nature* 494, 472–475. <https://doi.org/10.1038/nature11905>.
- Omondi, B.A., Latorre-Estivalis, J.M., Rocha Oliveira, I.H., Ignell, R., and Lorenzo, M.G. (2015). Evaluation of reference genes for insect olfaction studies. *Parasit. Vectors* 8, 243.
- Pfaffli, M.W. (2001). A new mathematical model for relative quantification in real-time RT-PCR. *Nucleic Acids Res.* 29, 45e–45. <https://doi.org/10.1093/nar/29.9.e45>.
- Pontes, G., Minoli, S., Insaurralde, I.O., de Brito Sanchez, M.G., and Barrozo, R.B. (2014). Bitter stimuli modulate the feeding decision of a blood-sucking insect via two sensory inputs. *J. Exp. Biol.* 217, 3708–3717. <https://doi.org/10.1242/jeb.107722>.
- Pontes, G., Pereira, M.H., and Barrozo, R.B. (2017). Salt controls feeding decisions in a blood-sucking insect. *J. Insect Physiol.* 98, 93–100. <https://doi.org/10.1016/j.jinsphys.2016.12.002>.
- Popescu, A., Couton, L., Almaas, T.J., Rospars, J.P., Wright, G.A., Marion-Poll, F., and Anton, S. (2013). Function and central projections of gustatory receptor neurons on the antenna of the noctuid moth *Spodoptera littoralis*. *J. Comp. Physiol. A Neuroethol. Sens. Neural Behav. Physiol.* 199, 403–416. <https://doi.org/10.1007/s00359-013-0803-0>.
- Reiter, S., Campillo Rodriguez, C., Sun, K., and Stopfer, M. (2015). Spatiotemporal coding of individual chemicals by the gustatory system. *J. Neurosci.* 35, 12309–12321. <https://doi.org/10.1523/jneurosci.3802-14.2015>.
- Riabinina, O., Task, D., Marr, E., Lin, C.-C.C., Alford, R., O'Brochta, D.A., and Potter, C.J. (2016). Organization of olfactory centres in the malaria mosquito *Anopheles gambiae*. *Nat. Commun.* 7, 13010. <https://doi.org/10.1038/ncomms13010>.
- Roper, S.D. (2015). The taste of table salt. *Pflügers Arch. Eur. J. Physiol.* 467, 457–463. <https://doi.org/10.1007/s00424-014-1683-z>.
- Scott, K. (2018). Gustatory processing in *Drosophila melanogaster*. *Annu. Rev. Entomol.* 63, 15–30. <https://doi.org/10.1146/annurev-ento-020117-043331>.
- Spector, A.C., Guagliardo, N.A., and St John, S.J. (1996). Amiloride disrupts NaCl versus KCl discrimination performance: implications for salt taste coding in rats. *J. Neurosci.* 16, 8115–8122. <https://doi.org/10.1523/jneurosci.16-24-08115.1996>.
- World Health Organization, 2020. Fact sheet, <https://www.who.int/news-room/fact-sheets/detail/vector-borne-diseases>.
- Yarmolinsky, D.A., Zuker, C.S., and Ryba, N.J.P. (2009). Common sense about taste: from mammals to insects. *Cell* 139, 234–244. <https://doi.org/10.1016/j.cell.2009.10.001>.
- Zeiner, R., and Tichy, H. (1998). Combined effects of olfactory and mechanical inputs in antennal lobe neurons of the cockroach. *J. Comp. Physiol. Sens. Neural Behav. Physiol.* 182, 467–473. <https://doi.org/10.1007/s003590050194>.
- Zeiner, R., and Tichy, H. (2000). Integration of temperature and olfactory information in cockroach antennal lobe glomeruli. *J. Comp. Physiol. A.* 186, 717–727. <https://doi.org/10.1007/s003590000125>.
- Zelle, K.M., Lu, B., Pyfrom, S.C., and Ben-Shahar, Y. (2013). The genetic architecture of degenerin/epithelial sodium channels in *Drosophila*. *G3 (Bethesda)* 3, 441–450. <https://doi.org/10.1534/g3.112.005272>.
- Zhang, Y.V., Ni, J., and Montell, C. (2013). The molecular basis for attractive salt-taste coding in *Drosophila*. *Science* 340, 1334–1338. <https://doi.org/10.1126/science.1234133>.

## STAR★METHODS

## KEY RESOURCES TABLE

REAGENT or RESOURCE	SOURCE	IDENTIFIER
<b>Chemicals, peptides and recombinant proteins</b>		
Adenosine 5'-triphosphate disodium salt hydrate	Sigma Aldrich	A26209
Amiloride hydrochloride hydrate	Sigma Aldrich	A7410
Anhydrous caffeine	Biopack	CAS# 58-08-2
Neurobiotin Tracer	Vector Laboratories	SP-1120
Dextran, Tetramethylrhodamine	ThermoFisher Scientific	D3308
Oregon Green-avidin 488 conjugate	Molecular probes	A6374
Triton X	Sigma Aldrich	X102
TRIzol RNA Isolation	ThermoFisher Scientific	10296010
Chloroform	Merck	288306
Ethanol	Merck	1009831000
Isopropanol	Merck	I9516
RQ1 RNase-Free DNase	Promega	M6101
Agarose Agargen	Laboratorios Espanagar	6108
SuperScriptSuperScript III Reverse Transcriptase	ThermoFisher Scientific	12574026
FastStart SYBR Green Master	Merck	4673484001
MEGAscript™ RNAi Kit T7	Thermo Fisher Scientific	AM1334
<b>Deposited data</b>		
Raw data	Mendeley Data	<a href="https://data.mendeley.com/datasets/sm4y3wmg3z/2">https://data.mendeley.com/datasets/sm4y3wmg3z/2</a> ; <a href="https://doi.org/10.17632/sm4y3wmg3z.2">https://doi.org/10.17632/sm4y3wmg3z.2</a>
<b>Experimental models: Organisms/strains</b>		
<i>Rhodnius prolixus</i>	Lab colony	N/A
<b>Oligonucleotides</b>		
Customized oligonucleotides for RT-PCR and qRT-PCR	Macrogen Inc.	
Customized oligonucleotides for dsRNAi synthesis	Macrogen Inc.	

## RESOURCE AVAILABILITY

## Lead contact

Further information and requests for resources and reagents should be directed to and will be fulfilled by the lead contact, Romina B. Barrozo ([rbarrozo@bg.fcen.uba.ar](mailto:rbarrozo@bg.fcen.uba.ar)).

## Materials availability

This study did not generate new unique reagents.

## Data and code availability

All data needed to evaluate the conclusions in the paper are present in the paper and/or the [supplemental information](#). All data have been deposited on Mendeley Data (<https://data.mendeley.com/datasets/sm4y3wmg3z/2>; <https://doi.org/10.17632/sm4y3wmg3z.2>) and are publicly available. Any additional information is available from the [lead contact](#) upon request.

This paper does not report original code.

## EXPERIMENTAL MODEL AND SUBJECT DETAILS

### Insects

Fifth-instar larvae and adults of *R. prolixus* were used throughout the experiments. Insects were reared at 28°C, ambient relative humidity (RH) and 12 h: 12h L/D cycle. Insects used in the experiments did not have access to food following ecdysis. Fifth-instar larvae were used for feeding assays and RNAi experiments 7 - 21 days post-ecdysis. Adults used for neuroanatomy experiments were 7 - 9 day-old post-ecdysis.

## METHODS DETAILS

### Feeding assays

Feeding behavior was examined using an artificial feeder described earlier (Pontes et al., 2014). Briefly, it consisted of a recipient (*i.e.* the feeder) filled with the appetitive solution (AS) with its lower opening closed with a latex membrane of 3.14 cm<sup>2</sup> (*i.e.* bite substrate mimicking the host skin). The AS consisted of a 0.001 M aqueous solution of adenosine 5'-triphosphate disodium salt hydrate (ATP) (Sigma Aldrich, St. Louis, US) and 0.15 M NaCl (Biopack, Buenos Aires, AR). Insects were placed individually inside a plastic vial. A piece of filter paper inside the plastic vial allowed bugs to reach the membrane of the feeder. The feeder containing the AS was heated to 35°C. The heat emitted by the recipient motivated the insects to approach the heated source (Flores and Lazzari, 1996; Guerenstein and Nuñez, 1994; Pontes et al., 2014).

Insects were weighed individually before (initial weight, *W<sub>i</sub>*) and after (final weight, *W<sub>f</sub>*) the feeding assay. Assays started when both containers, the plastic vial with the insect and the feeder with the heated AS, were put in contact and lasted for 10 min. Bugs had to pierce the membrane with their mouthparts to ingest the AS. A normalized weight gain was calculated as  $(W_f - W_i)/W_i$ . Due to the large variability of the ingested volumes across individuals, we considered those insects that ingested at least one time their initial weight to be effectively fed (Pontes et al., 2014). Consequently, the percentage of insects whose normalized weight gain was higher than 1 was calculated. Furthermore, a series of experiments were carried out in parallel to check biting events regardless of whether or not feeding occurred. Thus, the percentage of insects that extended their proboscis and bit the membrane was calculated. Experiments were carried out at the beginning of the scotophase when kissing bugs display their maximal motivation to feed (Barrozo et al., 2004; Bodin et al., 2008).

### Effect of salt concentration

Before reaching the AS, insects get in contact with the treated membrane by touching it both the antennae and tarsi. The bite membrane (3.14 cm<sup>2</sup>) was impregnated with 50 µL of NaCl or KCl at the following concentrations 0.15 M (0.0024 mmol cm<sup>-2</sup>, low-Na/low-K), 0.5 M (0.0079 mmol cm<sup>-2</sup>, mid-Na/mid-K), 1 M (0.016 mmol cm<sup>-2</sup>, high-Na/high-K) or with distilled water (no-Na/no-K, as control). This range of concentrations was chosen based on Masagué et al. (2020).

### Effect of amiloride

Amiloride hydrochloride hydrate (AMI) (Sigma Aldrich, St. Louis, US) was applied by allowing insects to walk freely for 1 min over a filter paper (12.5 cm<sup>2</sup>) coated with 50 µL of 0.001 M AMI (4.10<sup>-6</sup> mmol cm<sup>-2</sup>) (+AMI). This procedure allowed avoiding placing amiloride on the heated membrane preventing its potential heat-induced degradation. The control group (-AMI) consisted of insects exposed to a filter paper impregnated with distilled water. Once over the filter paper, the insect explored the substrate by touching it with both the antennae and the tarsi. Next, the feeding performance of insects to the AS was tested on the artificial feeder whose bite membrane was coated with high-Na/high-K or no-Na/no-K.

### Role of the antenna

The last third of the distal flagellomeres of both antennae were cut off 24 h before the feeding assays. The feeding performance to the AS was tested with bugs from the ablated group (-ANT) and intact ones (+ANT) as control. As previously, the bite membrane of the artificial feeder was coated with high-Na or no-Na.

### Electrophysiological recordings

Single-sensillum recordings (Hodgson et al., 1955) were carried out on the four most distal taste sensilla of the distal flagellomeres, previously characterized by Pontes et al. (2014) (shown in Figure 2A). Insects were immobilized inside a plastic pipette, with both antennae kept outside and fixed. Insects were grounded via

insertion of an Ag/AgCl wire to the anus (reference electrode), and a glass capillary (20  $\mu\text{m}$  in diameter at the tip) holding an Ag/AgCl wire inside served for both stimulus presentation and GRN response recording. Stimulus presentation lasted for 2 s and started once the glass capillary covered the tip of a single sensillum. The interval between subsequent stimulus presentations was 2 min. The biological signals were amplified, filtered (preamplifier: gain $\times$ 10, TastePROBE DTP-02, Syntech, Kirchzarten, DE; amplifier: gain $\times$ 100, eighth-order Bessel, pass-band filter: 10–3000 Hz, Dagan Ex1, Minneapolis, US), digitized (sampling rate: 10 kHz, 16 bits, Data acquisition module DT9803, Data Translation, Massachusetts, US) and stored in a PC. Spike detection and sorting were performed offline using the dbWave software (Marion-Poll, 1996). The number of action potentials elicited during the first second of recording was quantified.

### *Physiological responses of GRNs*

Taste sensilla were stimulated with 0.0001, 0.001, 0.01, 0.1, 0.2 and 0.5 M NaCl or KCl. Salt crystallization at the tip of the glass capillary impeded testing doses higher than 0.5 M. 0.1 mM anhydrous caffeine (Biopack, Buenos Aires, AR) in 1 mM NaCl was tested (Figure S2). Spike frequencies were calculated for each stimulation. Additionally, the firing profile over time to 0.01 M (Figures 2D and 2E) and 0.5 M (Figure S3) NaCl/KCl were characterized for the different GRN types. To do this, the number of spikes per 100 ms bin was calculated across the 2 s of each recording/GRN and averaged for neurons of the same type. Peri-stimulus-time histograms allowed visually analyzing the temporal firing pattern of the two GRN types identified.

### *Effect of amiloride on GRNs*

Taste sensilla of the distal flagellomeres (Figure 2A) were treated with 0.001 M AMI by gently touching them with an impregnated toothpick. Two control groups were required, one group with sensilla treated with a toothpick coated with distilled water (-AMI) and the other with sensilla treated with a dry toothpick (MCt). The latter being a mechanical control for the procedure. It is expected that touching the sensilla with a toothpick coated with distilled water (solvent used for AMI) or kept dry would not affect the physiology of GRNs, as shown in Figure S5. Afterward, the firing responses of GRNs to 0.01 or 0.2 M NaCl or KCl were recorded. These two salt concentrations chosen represented the detection threshold and saturation of cellular responses. The effect of AMI was evaluated for the same sensilla over time. For this, GRN firing responses to 0.01 M NaCl/KCl (Figures 2H and 2I) and to 0.2 M NaCl/KCl (Figure S4) were recorded at 0, 10, 20 and 30 min post-treatment.

### *Physiological responses of GRNs after gene silencing*

The firing activity of GRNs to 0.01 M NaCl and KCl was recorded for non-injected and dsRNA injected insects (see below). This salt concentration elicited the optimal neuronal response, in which both GRNs have reached or are close to the saturation limit of their response to NaCl or KCl.

### **Tracing of GRNs**

Two neuronal tracers were used: neurobiotin (1% in 0.25 M KCl, Neurobiotin Tracer®, Vector Laboratories, Burlingame, US) and rhodamine (1% in distilled water, Dextran, Tetramethylrhodamine, 3000 MW, Anionic, Lysine Fixable, Thermo Fisher, Massachusetts, US). To visualize the brain structures innervated by the afferent antennal neurons, bilateral anterograde mass fills of the antennae were performed using neurobiotin (as shown in Barrozo et al., 2009). To do this, the dye was applied to each antenna after sectioning at the pedicel level.

To restrict backfills, both tracers were applied to the 4 distal taste sensilla of the distal flagellomeres (Figure 2A). The tips of the taste sensilla were pre-cut to allow the dye to penetrate the gustatory neurons. Thereafter, cut sensilla were immersed for 6 min in distilled water. Rhodamine was applied simultaneously on the 4 taste sensilla, by inserting the 4 sensilla in glass capillaries containing the dye, in 12 insects. To assure that only GRNs originating in the 4 distal sensilla became stained, the same procedure was exactly performed simultaneously to both antennae of the same animal. However, while the 4 taste sensilla of one antenna were cut, the sensilla of the other antenna remained intact. Additionally, stainings on a single sensillum were carried out by using neurobiotin as a neuronal marker in 19 animals. The rationale behind this experiment was to refine the tracing of the GRNs housed in a single taste sensillum to the brain.

Neurobiotin and rhodamine were allowed to migrate to the brain for 12 h at room temperature or 48 h at 4°C, respectively. Following tracers' migration times, the insects were sacrificed and the brains were dissected in Millonig's buffer and fixed in 4% paraformaldehyde overnight at 4°C. Neurobiotin-stained brains were dehydrated and rehydrated in an alcohol series (50%, 70%, 90%, 100%) and propylene oxide and next incubated in Oregon Green-avidin (Oregon green® 488 conjugate, Molecular probes, Oregon, US) with 0.2% Triton X and 1% BSA overnight at 4°C (Barrozo et al., 2009). Subsequently, neurobiotin-treated brains were rinsed in Millonig's buffer and dehydrated in the alcohol series. Rhodamine-treated brains were rinsed in Millonig's buffer and dehydrated through sequential baths in the same ethanol series and propylene oxide. Then, all brains were cleared and mounted in methyl salicylate. Whole mounts were optically sectioned and scanned with a laser scanning confocal microscope (Olympus FV1000/BX51).

### Antennal expression of PPKs

One hundred distal flagellomeres from fifth-instar larvae were excised, and a total of three replicates were prepared. Samples were manually homogenized using sterilized pestles and total RNA was extracted using 500  $\mu$ L of TRIzol® Reagent (Life Technologies, Carlsbad, US) according to the manufacturer's instructions. The concentration of RNA extraction products was determined using a Qubit® 2.0 fluorometer (Life Technologies, Carlsbad, US). All samples were treated with RQ1 RNase-Free DNase (Promega, Fitchburg, US). Treated RNA (11  $\mu$ L per sample) was used to produce cDNA through the Super-Script III Reverse Transcriptase (Life Technologies, Carlsbad, US) and a 1:1 mix of Random Hexamers and 10  $\mu$ M Oligo(dT) 20 primers to a final volume of 20  $\mu$ L. For qPCR reactions, 7.5  $\mu$ L of FastStart SYBR Green Master (Hoffmann-La Roche, Basel, SW) were used in the reaction that also contained 0.3  $\mu$ L of a 10  $\mu$ M primer solution and 1  $\mu$ L of cDNA sample into a final volume of 15  $\mu$ L. The reactions were conducted using the Mini Opticon Real-Time PCR Detector Separate MJR (Bio-Rad Laboratories, California, US) under the following conditions: 10 min cycle at 95°C, followed by 40 cycles of 20 s at 95°C, 20 s at 60°C and 30 s at 72°C. Real-time data were collected through the CFX Manager 3.0 software (Bio-Rad Laboratories, California, US). After qPCR reactions, melting curve analyses were performed to confirm reaction specificity. Non-template controls (NTC) were included for each primer set to verify the absence of exogenous DNA. To confirm amplicon sizes, qPCR products were run on a 2% agarose gel stained with ethidium bromide. NTCs were also included in the agarose gel.

### RNA interference

#### Double-strand RNA synthesis

Double strand RNAs (dsRNA) of *RproPPK014276* and *RproPPK28* were synthesized by amplification of antennal cDNA using PCR. The ampicillin resistance beta-lactamase gene ( $\beta$ -lact) of *Escherichia coli* was also amplified from the pBluescript SK plasmid as control of dsRNA injection (see below). PCR was carried out by using specific primers conjugated with 20 bases of the T7 RNA polymerase promoter (Table S1). PCR products, 200, 202 and 253 bp for *RproPPK014276* and *RproPPK28* and  $\beta$ -lact, respectively, were used as templates for dsRNA synthesis using the MEGAscript™ T7 RNAi Kit (Thermo Fisher Scientific, Massachusetts, US). Each PCR fragment was sequenced and their sequences were identical to the expected fragments. After synthesis, the purity and integrity of dsRNA were confirmed by running a 1.5% agarose gel and quantified using NanoDrop™ (Thermo Fisher Scientific, Massachusetts, US). The specificity of the dsRNA for each PPK was validated *in silico* using BLASTn searches against the *R. prolixus* genome sequence, each dsRNA sequence showed a unique and complete hit against its target sequence.

#### ds-RNA injection

Insects were randomly separated into 4 experimental groups for dsRNA injections. Two groups of insects were injected with the dsRNAs against the genes of interest: dsRNA-*RproPPK014276* and dsRNA-*RproPPK28*. A third group was injected with the dsRNA of  $\beta$ -lact, representing a control for dsRNA injection: dsRNA-ctrl. A microliter syringe (World Precision Instruments, Florida, US) was used to inject 2  $\mu$ L of 1.25  $\mu$ g/ $\mu$ L dsRNA diluted in PBS1X into the thoracic hemolymph of insects. The fourth group of insects was maintained intact (non-injected group) to control for potential effects of the injection procedure. Eleven days after dsRNA injection, insects of each group were tested for qPCR verification of gene expression knockdown, in electrophysiological recordings or behavioral assays (see below).

To evaluate the efficacy of PPK knockdown, 20 antennae per group were excised (6 to 12 replicates per treatment). Total RNA was extracted as previously described using 250  $\mu$ L of TRIzol® Reagent, treated

with RQ1 RNase-Free DNase (Promega, Fitchburg, US) and used to synthesize cDNA using the SuperScript III Reverse Transcriptase (Thermo Fisher Scientific, Massachusetts, US), to a final volume of 30  $\mu$ L. qPCR reactions were performed as described for expression profile experiments, except for the instrument that was an AriaMx Real-Time qPCR System (Agilent, California, US). The relative gene expression was calculated using the  $2^{-\Delta\Delta C_t}$  method (Pfaffl, 2001). First, the gene expression for each condition was normalized using the geometric mean of two reference genes that were previously reported to have a stable expression in *R. prolixus* antennae, *RproGADPH* and *RproG6PDH* (Omondi et al., 2015). Subsequently, this relative expression was normalized using the expression of the non-injected group as reference.

### Behavioral response after gene silencing

A simultaneous two-choice preference arena was used (Masagué et al., 2020). It consisted of a rectangular acrylic box (10  $\times$  5 cm) divided into two equal zones of 25 cm<sup>2</sup> each. The substrate (filter paper) of one zone was coated with 100  $\mu$ L distilled water (no-Na/no-K), while that of the other zone received either 100  $\mu$ L of 1 M NaCl (high-Na) or KCl (high-K) (i.e. 0.004 mmol cm<sup>-2</sup>). One insect was placed inside an inverted recipient at the center of the arena for 1 min, to acclimate to the experimental condition. Following this time, the insect was released and its preference was recorded for 4 min using an infrared-sensitive video camera connected to a digital recorder. A preference index (PI) was calculated as the difference between the time spent in each zone of the arena divided by the total experimental time. PIs near 0 indicate a lack of preference. PIs close to -1 or 1 show preference for either zone of the arena. All experiments were carried out in a dark room during the scotophase (see above).

## QUANTIFICATION AND STATISTICAL ANALYSIS

### Feeding assays

Data were analyzed statistically using contingency tables of independence through a Pearson's Chi-squared test ( $\chi^2$ ), followed by individual *post hoc* comparisons. To avoid experiment-wise errors, the  $\alpha$  value (0.05) was corrected with the Bonferroni correction ( $\alpha' = \alpha/k$ ,  $k$  = number of comparisons). The standard errors of percentages were calculated as  $\sqrt{p(1-p)/N}$ ;  $p$ : proportion of response;  $N$ : number of animals tested. 20 to 36 replicates were carried for each condition.

### Electrophysiological recordings

Logarithmic salt concentration and mean firing frequencies of GRNs were fitted to a 3 parameter dose-response curve, and the best-fit was examined through Goodness of fit and  $R^2$  values ( $R^2 > 0.94$ ). Except for S2-GRN stimulated with KCl ( $R^2 = 0$ ), no significant deviations from the model were detected ( $p > 0.8$ ). The effect of AMI on the firing frequency of the GRNs was statistically analyzed using a one-tailed Wilcoxon matched-pairs signed-rank test to compare responses to the salt concentrations (Figures 2F and 2G) or at post-application times (i.e. 0, 10, 20, 30 min) (Figures 2H, 2I, and S4) or caffeine stimulation (Figure S2). The  $\alpha$  value (0.05) was corrected with the Bonferroni correction in Figures 2H, 2I, and S4, where  $k = 4$  and  $\alpha' = 0.0125$ . The effect of gene silencing was assessed by using the Kruskal-Wallis test followed by *post hoc* Dunn's comparisons on the responses of GRNs to salts. 6 to 27 sensilla were tested for each experimental condition.

### Gene expression

The relative expression levels of knockdown genes were statistically compared by using the Kruskal-Wallis test followed by *post hoc* Dunn's comparisons. 6 to 12 replicates were carried out per treatment.

### Two-choice behavioral assays

The PIs obtained for each animal of non-injected and dsRNA injected groups were statistically compared against a PI value of 0 (i.e. no preference) by using one-sample *t*-tests. 24 to 28 replicates were carried out for each experimental condition.